

# Quasiparticle band structures in transitional nuclei

*Proceedings of the DAE Symp. on Nucl. Phys.* 57 (2012) G. H. Bhat, J. A. Sheikh<sup>1</sup>, P. A. Ganai<sup>1,3</sup>, Yang Sun<sup>4</sup>

<sup>1</sup>Department of Physics, University of Kashmir, Srinagar, 190 006, India

<sup>2</sup>Department of Physics and Astronomy,  
University of Tennessee, Knoxville, TN 37996, USA

<sup>3</sup>Department of Physics, NIT, Srinagar 190 006

<sup>4</sup>Department of Physics, Shanghai Jiao Tong University,  
Shanghai 200240, People's Republic of China\*

(Dated: June 27, 2012)

268

Major advances in the experimental techniques have made it feasible to perform detailed measurements of atomic nuclei at the extremes of angular-momentum, isospin and stability. Detailed spectroscopic studies have provided new insights in our understanding of nuclear many-body problem. Band structures have been observed up to very high angular-momentum and far from the valley of stability. For instance, in the deformed nucleus Dy, sixty bands have been reported. The classification and the interpretation of these rich band structures is a challenge to nuclear theory. The three modes of excitations of rotational, vibrational and quasi-particle constitute the primary origin of the observed bands in nuclei. In spherical nuclei, the energy spectrum is primarily built on the quasi-particle excitations. In well deformed nuclei, rotational bands are observed and are classified using the Nilsson scheme. On the other hand, in transitional nuclei the excitation spectrum is quite rich which depicts interplay of all the three modes of excitations [1, 2]. It is quit evident that in transitional nuclei there are two low-lying quadrupole vibrational modes of motion. These are ascribed to  $\beta$  and  $\gamma$ -vibrations. The mode of vibration with no component of angular momentum along the symmetry axis ( $K = 0$ ) are called  $\beta$ -vibrations, which can be well understood with axial symmetry, on the other hand the mode of vibration with component of angular momentum along the symmetry axis ( $K = 2$ ) are called  $\gamma$ -vibrations and this mode of vibration can be explained by breaking the axial symmetry in the Nilsson potential. Further, the bandhead energy of  $\beta$  and  $\gamma$ -vibrations and lowly-lying octupole vibrational bands are almost located at nearly the same excitations. Therefore, the closeness in the phonon excitation energies associated with all of these collective modes makes the complex band interactions. These structures, therefore, couple  $\gamma$ -vibration to qp-excitations, based on which rotational bands are built. Thus, these bands have characteristics of all three excitation modes in the nuclei and are, therefore, the best places to show up the interplay among them. The recent developments in triaxial projected shell model (TPSM) approach have greatly enhanced the model predictability and may provide new insights into the observed bands with unknown structures.

Thanks, to the experimental efforts for The low-lying  $K = 3^+$  band, which subsequently decays to both the  $\gamma$ -vibrational and the ground-state bands. The occurrence of appreciable K-

forbidden  $E2$  transitions from the  $K = 3^+$  to the ground-state band is attributed to mixing with the  $K = 2^+$  band, caused by the interaction between the  $\gamma$ -vibrational and the quadrupole vibrational motions. Surprising observation of the appreciable population of the  $K = 3^+$  band in  $^{174}\text{Hf}$  and  $^{172}\text{yb}$  [3, 4], the nature of which has remained unresolved, and its subsequent decay to both the  $\gamma$ -vibrational and the ground-state bands. Since the dominant excitation path in Coulomb excitation is via  $E2$  transitions, it is difficult to explain the population of the  $K = 3^+$  band without invoking a K mixing scheme. Therefore, TPSM is appreciable tool to provide the reasonable explanation on K mixing scheme.

For even-even systems, the TPSM basis are composed of projected 0-qp state (or qp-vacuum  $|\Phi\rangle$ ), 2-proton, 2-neutron, and 4-qp configurations, i.e.,

$$\begin{aligned} & \hat{P}_{MK}^I |\Phi\rangle; \\ & \hat{P}_{MK}^I a_{p_1}^\dagger a_{p_2}^\dagger |\Phi\rangle; \\ & \hat{P}_{MK}^I a_{n_1}^\dagger a_{n_2}^\dagger |\Phi\rangle; \\ & \hat{P}_{MK}^I a_{p_1}^\dagger a_{p_2}^\dagger a_{n_1}^\dagger a_{n_2}^\dagger |\Phi\rangle, \end{aligned} \quad (1)$$

where the three-dimensional angular-momentum operator [10] is given by

$$\hat{P}_{MK}^I = \frac{2I+1}{8\pi^2} \int d\Omega D_{MK}^I(\Omega) \hat{R}(\Omega), \quad (2)$$

with  $\hat{R}(\Omega)$  being the rotation operator and  $D_{MK}^I(\Omega)$  the  $D$ -function. It is important to note that for the case of axial symmetry, the qp-vacuum state has  $K = 0$  where as in the present case of triaxial deformation, the vacuum state  $|\Phi\rangle$ , as well as any configuration in (1), is a superposition of all possible  $K$ -values.

As in the earlier TPSM calculations, we use triaxial Nilsson mean-field Hamiltonian, which is obtained by using the Hartree-Fock-Bogoliubov (HFB) approximation, is given by

$$\hat{H}_N = \hat{H}_0 - \frac{2}{3}\hbar\omega \left\{ \varepsilon \hat{Q}_0 + \varepsilon' \frac{\hat{Q}_{+2} + \hat{Q}_{-2}}{\sqrt{2}} \right\}. \quad (3)$$

Here  $\hat{H}_0$  is the spherical single-particle Hamiltonian, which contains a proper spin-orbit force. The interaction strengths are taken as follows: The  $QQ$ -force strength  $\chi$  is adjusted such that the physical quadrupole deformation  $\varepsilon$  is obtained as a result of the self-consistent mean-field HFB calculation [10]. The monopole pairing strength  $G_M$  is of the standard form

$$G_M = (G_1 \mp G_2 \frac{N-Z}{A}) \frac{1}{A} (\text{MeV}), \quad (4)$$

\*gwhr.bhat@gmail.com

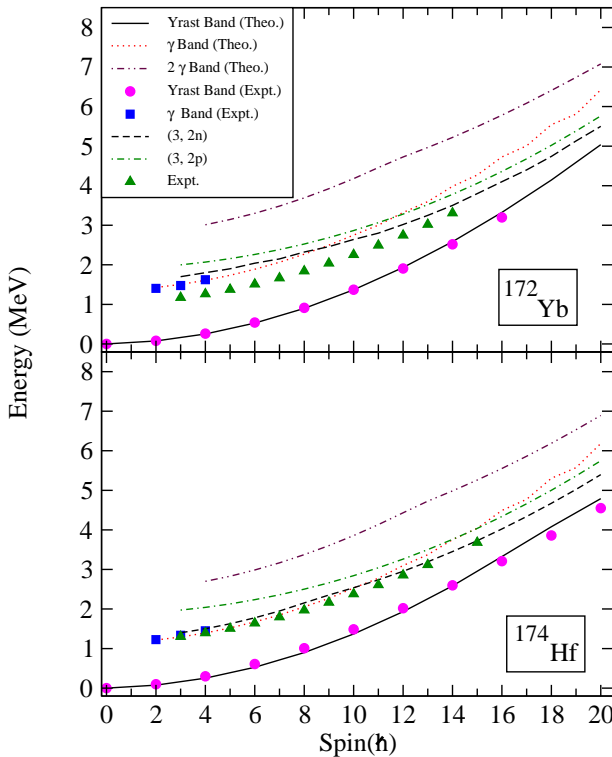


FIG. 1. Detailed comparison of the  $K=3$  band structure  $^{172}\text{Yb}$  and  $^{174}\text{Hf}$  isotope.

where  $-$ ( $+$ ) is neutron (proton). In the present calculation, we use  $G_1 = 20.12$  and  $G_2 = 13.13$ , which approximately reproduce the observed odd-even mass difference in this region. This choice of  $G_M$  is appropriate for the single-particle space employed in the model, where three major shells are used for each type of nucleons ( $N = 3, 4, 5$  for protons and  $N = 4, 5, 6$  for neutrons). The quadrupole pairing strength  $G_Q$  is assumed to be proportional to  $G_M$ , and the proportionality constant being fixed as 0.16. These interaction strengths are consistent with those used earlier for the same mass region [6–8]. This choice of  $G_M$  is appropriate for the single-particle space employed in the model, where three major shells are used for each type of nucleons ( $N = 3, 4, 5$  for protons and  $N = 4, 5, 6$  for neutrons). In present calculations, the deformation parameters  $\epsilon$  used are from Ref. [5]. The chosen values of  $\epsilon$  for the present calculation are those from the measured quadrupole deformations of the nuclei, as is done in the previous projected shell model analysis. The triaxial parameter  $\epsilon'$  is chosen so

that the calculated energy of the  $\gamma$ -bandhead reproduces the measured value. To further clarify that the  $\epsilon'$  values used in the present work are realistic, we have calculated the ground-state energies as a function of  $\epsilon'$ . These energy surface calculations clearly depict a minimum for the values used in the present work.

In the present work, Fig. 1 depicts the calculated bands after diagonalization and also displays the corresponding available experimental data. It is important to point out that, although, the bands in Fig. 1 are labeled as  $\gamma$ ,  $\gamma\gamma$ , and  $K = 3$ , bands, these are only the dominant components in the wavefunction. The projected states after diagonalization are in general mixed. In particular, 2-qp  $K = 3$  band has a significant contribution from 0-qp  $K = 2$  configuration at higher angular-momenta. It is quite clear from Fig. 1 that there is a strong coupling interaction between the quasiparticle excitations with  $\gamma$ -vibration in isotonic chain of  $^{174}\text{Hf}$  and  $^{172}\text{Yb}$ . Fig. 1 depicts the calculated bands after diagonalization and also displays the corresponding available experimental data. The calculated  $K = 3$  2-qp neutron band in  $^{174}\text{Hf}$  agrees quite well with the experimental band, however, in  $^{172}\text{Yb}$  at low spin region some discrepancies are quite evident. There could be several reasons for these discrepancies. The bulk of the discrepancy could be attributed to the fixed mean-field assumed in the present study. The Nilsson potential is chosen for the mean-field and is determined by the input deformation parameters,  $\epsilon$  and  $\epsilon'$ . The pairing potential, on the other hand, is obtained from the monopole interaction using the BCS ansatz. In a more accurate self-consistent treatment, projection before variation, the mean-field and the pairing potential are known to vary with qp-excitation and angular-momentum. However, a good agreement  $^{174}\text{Hf}$  and  $^{172}\text{Yb}$  can be obtained by increasing the quadrupole deformation. It is worth to mention here that, although the axial deformation is important for the  $K = 3$  band to appear, the strong mixing with  $\gamma$ -degree of freedom is crucial to explain its excitation and the rotational behavior. Therefore, this band has mainly a structure of triaxially deformed 2-qp state projected to the  $K = 3$  component. It is interesting to note that there is strong crossing region of the two bands ( $\gamma$  and  $K = 3$  band around spin 12), and is enhanced by E2 transition implying a strong mixing between the quasiparticles and the  $\gamma$ -vibration. It has been further shown that the detailed structure and position of the  $K = 3$  band depend sensitively on the shell filling. The prediction of systematic appearance of two  $K = 3$  bands with proton and neutron structures at higher spin, close to the yrast line, awaits experimental confirmation [11].

- 
- [1] A. Bohr and B. R. Mottelson, *Nuclear Structure*, Vol. II (Benjamin Inc., New York, 1975).
- [2] A. Bohr and B. R. Mottelson, Phys. Scr. **25**, 28 (1982).
- [3] B. Singh, Nucl. Data Sheets **75**, 199 (1995).
- [4] E. Browne, Nucl. Data Sheets **62**, 1 (1991).
- [5] S. Raman, et al., Atom. Data Nucl. Data Tables **36**, 1 (1987).
- [6] J. A. Sheikh, G. H. Bhat, et al., Phys. Rev. C **77**, 034313 (2008).
- [7] J. A. Sheikh, G. H. Bhat, R. Palit, Z. Naik, and Y. Sun, Nucl. Phys. A **824**, 58 (2009).
- [8] J. A. Sheikh, G. H. Bhat, Y. Sun, and R. Palit, Phys. Lett. B **688**, 305 (2010).
- [9] P. Boutachkov, et al., Eur. Phys. J. A **15**, 455 (2002).
- [10] K. Hara and Y. Sun, Int. J. Mod. Phys. E **4**, 637 (1995).
- [11] J. A. Sheikh, G. H. Bhat, et. al., Phys. Rev. C **84**, 054314 (2011).